Bulletin of the Seismological Society of America, Vol. 102, No. 6, pp. 2781–2788, December 2012, doi: 10.1785/0120120068

Short Note

Spatial Correlation of Spectral Acceleration in European Data

by Simona Esposito and Iunio Iervolino

Abstract Quantification of regional seismic risk is based on spatially correlated random fields and requires modeling of the joint distribution of ground-motion intensity measures at all sites of interest. In particular, when a portfolio of buildings or a transportation/distribution network (lifeline) is of concern, correlation models for elastic spectral acceleration (SA) may also be required in order to estimate the expected loss in case of seismic events. The presented study focuses on semi-empirical estimation of spatial correlation as a function of intersite separation distance. In fact, this paper complements, and is based on, preceding work of the authors referring to spatial correlation of peak ground acceleration and velocity (Esposito and Iervolino, 2011). The evaluation of correlation for ground-motion residuals was performed on data from multiple earthquakes, considering different ground-motion prediction equations fitted to the same records. Correlation analyses, carried out through geostatistical tools, considered two datasets: the Italian Accelerometric Archive and the European Strong-Motion Database. Results appear generally consistent with previous research on the same topic. Finally, simple relationships providing the correlation range of intraevent residuals of SA, as a function of structural period, were derived for each dataset. The developed models are useful for earthquake engineering applications where spatial correlation of peak ground motion is required.

Introduction

Assessment of spatial correlation of ground-motion intensity measures (IMs) has become a relevant topic in seismic-risk analysis. The importance of modeling such phenomena is due to the requirement to extend risk assessment, usually related to site-specific structures, to spatially distributed systems, such as building portfolios and lifelines. In particular, on the hazard side, probabilistic seismic hazard analysis (McGuire, 2004) involves ground-motion prediction equations (GMPEs), which provide probabilistic distribution of the chosen IM (e.g., peak ground acceleration [PGA], peak ground velocity [PGV], and elastic spectral acceleration [SA]) conditional on earthquake magnitude, source-to-site distance, and other parameters, such as local geological conditions. Since GMPE residuals are spatially correlated (e.g., Boore *et al.*, 2003), neglecting such a correlation may bias the loss assessment of distributed systems (e.g., Esposito, 2011).

In the literature, several spatial-correlation models for different ground-motion parameters are available (e.g., Goda and Hong, 2008; Jayaram and Baker, 2009; Sokolov *et al.*, 2010). These models depend on intersite separation distance and provide the limit at which correlation may be technically considered to be lost (i.e., the distance beyond which intraevent residuals of IMs may be considered uncorrelated).

Herein, evaluation of the spatial correlation for SA (5% damped) residuals is carried out using two datasets: the Italian Accelerometric Archive (ITACA), and the European Strong-Motion Database (ESD). Residuals are computed using GMPEs by Bindi *et al.* (2011) and Akkar and Bommer (2010); only the records used to develop the considered GMPEs are employed to estimate spatial correlation.

The analysis of correlation was performed through geostatistical tools, pooling data from multiple events to fit a unique model based on working hypotheses, and findings of Esposito and Iervolino (2011) and Esposito *et al.* (2010). In fact, this paper complements the preceding work on spatial correlation of PGA and PGV using European multievent data.

The presentation of the study in the following is structured such that the first part briefly describes the framework adopted to estimate correlation (yet for a more comprehensive discussion, the reader should refer to Esposito and Iervolino, 2011). Subsequently, the working assumptions and a description of the considered datasets are given. Then, results of estimation of correlation ranges for SA at 7 structural periods, ranging from 0.1 s to 2 s for the Italian dataset, and at 9 periods, ranging from 0.1 s to 2.85 s for the European dataset, are presented. Finally, simple linear relationships for the correlation length as a function of structural

period are derived, discussed, and compared with other models.

Modeling Spatial Correlation of Ground Motion Intensity Measures

Geostatistical Framework

Spatial-correlation models provide the basic measure of spatial continuity of a random field. Regarding the spatial modeling of IMs for earthquake engineering purposes, the literature is mostly based on the estimation of correlation between residuals of ground-motion parameters at two different sites through the use of geostatistical tools. In particular, GMPEs generally model the logarithms of SA for a specific structural period T and related heterogeneity at a site p due to earthquake j as in

$$\log \mathrm{SA}(T)_{pj} = \overline{\log \mathrm{SA}(T)_{pj}}(M, R, \underline{\theta}) + \eta_j + \varepsilon_{pj}, \qquad (1)$$

where $\overline{\log \mathrm{SA}(T)_{pj}}(M, R, \underline{\theta})$ is the mean of the logarithms of SA conditional on parameters such as magnitude (M), source-to-site distance (R), and others ($\underline{\theta}$); η_j denotes the interevent residual, which is a constant term for all sites in a given earthquake and represents a systematic deviation of the mean of the specific seismic event; finally, ε_{pj} is the intraevent variability of ground motion. ε_{pj} and η_j are usually assumed to be independent random variables, normally distributed with zero mean and standard deviation σ_{intra} and σ_{inter}, respectively. Consequently, $\log \mathrm{SA}(T)_{pj}$ is modeled as a normal random variable with mean $\overline{\log \mathrm{SA}(T)_{pj}}(M, R, \underline{\theta})$ and standard deviation σ_T, where $\sigma_T^2 = \sigma_{\mathrm{inter}}^2 + \sigma_{\mathrm{intra}}^2$.

If hazard assessment at two or more sites at the same time is of concern, the joint probability density function for the logarithms of IM at all locations can be conveniently modeled with a multivariate normal distribution (e.g., Jayaram and Baker, 2008). In this case, it is assumed that the logarithms of IM form a Gaussian random field (GRF), defined as a set of random variables, one for each site $\mathbf{u}$ in the study area $S \in R^2$. In particular, ground-motion parameters at n spatial locations $\mathbf{u_p}$, $\{p = 1, \cdots, n\}$, are modeled as a collection of random variables characterized by a mean vector provided by the GMPE and a covariance matrix, Σ, defined as in

$$\Sigma = \sigma_{\mathrm{inter}}^2 \cdot \begin{bmatrix} 1 & 1 & \cdots & 1 \\ 1 & 1 & \cdots & 1 \\ \vdots & \vdots & \ddots & \vdots \\ 1 & 1 & \cdots & 1 \end{bmatrix} + \sigma_{\mathrm{intra}}^2 \cdot \begin{bmatrix} 1 & \rho(h_{12}) & \cdots & \rho(h_{1n}) \\ \rho(h_{21}) & 1 & \cdots & \vdots \\ \vdots & \vdots & \ddots & \vdots \\ \rho(h_{n1}) & \rho(h_{n2}) & \cdots & 1 \end{bmatrix}, \qquad (2)$$

where the first term produces perfectly correlated interevent residuals (Malhotra, 2008), while the second term (symmetrical) produces spatially correlated intraevent residuals. In equation (2), such a correlation is only a function of the separation distance h (under the hypothesis of second-order stationarity and isotropy of the GRF); that is, the spatial heterogeneity does not depend on the direction considered.

The covariance matrix typically depends on parameters obtained from a non-negative definite spatial parametric covariance model (Cressie, 1993). In this work, as also assumed in Esposito and Iervolino (2011), spatial correlation was estimated using all data available from different earthquakes and regions (deemed homogeneous) differently from studies focusing on earthquake-specific data (e.g., Jayaram and Baker, 2009).

Semivariograms and Correlation Functions

A common tool to quantify the variability of spatial data is the semivariogram, $\gamma_j(h)$. It is used to model the covariance structure of GRF through mathematically tractable functions fitted to empirical observations. Under the hypothesis of second-order stationary and isotropy mentioned above, it is defined as in

$$\gamma_j(h) = \mathrm{Var}(\varepsilon_j) \cdot [1 - \rho_j(h)], \qquad (3)$$

where $\mathrm{Var}(\varepsilon_j)$ is the homoscedastic variance of intraevent residuals and $\rho_j(h)$ denotes the spatial correlation coefficient between intraevent residuals at two generic sites separated by h distance.

The estimation of correlation based on semivariograms usually develops in three steps:

1. computing the empirical semivariogram[1], $\hat{\gamma}(h)$;
2. choosing a functional form for curve fitting;
3. estimating the parameters of the chosen function-fitting empirical data.

Regarding point (1): empirical semivariograms are computed as a function of site-to-site separation distance, with different possible estimators. The classical estimator is the method-of-moments (Matheron, 1962), which is defined, for an isotropic random field, as in

$$\hat{\gamma}(h) = \frac{1}{2 \cdot |N(h)|} \cdot \sum_{N(h)} [\varepsilon(\mathbf{u} + h) - \varepsilon(\mathbf{u})]^2, \qquad (4)$$

where $\varepsilon(\mathbf{u} + h) - \varepsilon(\mathbf{u})$ is the difference between intraevent residuals at sites separated by h distance value, $N(h)$ is the set of pairs of sites, separated by the same h distance in the dataset, at which the residuals of interest are measured, and $|N(h)|$ is the cardinal of $N(h)$.

[1]Assuming a common semivariogram for different events, that is, invariant through earthquakes, allows us to neglect for subscript j in the following equations.

Since this estimator can be badly affected by atypical observations (Cressie, 1993), Cressie and Hawkins (1980) proposed a more robust, in the statistical sense (i.e., less sensitive to outliers) estimator, equation (5). Both estimators are used in the following for the evaluation of intraevent spatial correlation of SA(T),

$$\hat{\gamma}(h) = \frac{1}{2} \cdot \left\{ \left[\frac{1}{|N(h)|} \cdot \sum_{N(h)} |\varepsilon(\mathbf{u}+h) - \varepsilon(\mathbf{u})|^{0.5} \right]^4 \Big/ \times \left(0.457 + \frac{0.494}{|N(h)|} \right) \right\}. \quad (5)$$

To compute the empirical semivariogram, it is necessary, when dealing with earthquake records, to define tolerance bins around each possible h value (this allows to divide data in classes, based on a similar concept of histograms to fit known probabilistic models to normalized observed frequency). The selection of distance bins has important effects: if the size is too large, correlation at short distances may be masked; conversely, if it is too small, empty bins, or bins with small numbers of samples, may lead to poor estimates. A rule of thumb is to choose the maximum bin size as a half of the maximum distance between sites in the dataset and to set the number of bins so that there are at least 30 pairs per bin (Journel and Huijbregts, 1978).

Point (2), concerning the interpretation of the experimental semivariogram, consists in the identification of a model among the family of functions able to capture and emulate its trend. The three basic stationary and isotropic models are exponential, spherical, and Gaussian (Goovartes, 1997). In particular, the exponential model, which is the most common one in literature, is described as

$$\gamma(h) = c_0 + c_e \cdot (1 - e^{-3 \cdot h/b}), \quad (6)$$

where c_0 is the nugget, that is, the limit value of the semivariogram when h tends to zero, c_e is the sill, or the population variance of the random field (Barnes, 1991), and b is the practical range, or the correlation length, defined as the intersite distance at which $\gamma(h)$ is equal to 95% of the sill, or in other words, the distance at which the correlation may be considered technically lost and residuals of ground-motion intensity may be considered independent (under the GRF assumption).

Regarding point (3), several goodness-of-fit criteria have been proposed in geostatistical literature to find the best parametric model. Studies dealing with earthquake data sometimes use visual or trial-and-error approaches in order to appropriately model the semivariogram structure at short site-to-site distances, where engineering significance is more important (Jayaram and Baker, 2009). In this work, experimental semivariograms are fitted using recursively the least squares method (LSM) on data obtained with the robust estimator (to follow).

Estimating Correlation on Multievent Data

Empirical semivariograms are computed starting from normalized intraevent residuals for a single earthquake j and a site p, as $\varepsilon^*_{pj} = \varepsilon_{pj}/\sigma_p$, where σ_p is the standard deviation of the intraevent residual at the site p (in the study, the intraevent standard deviation is common for all sites, consistent with GMPEs used to compute residuals). The standardization enables one to avoid the estimation of the sill, as it should be equal to one; therefore, equation (3) becomes

$$\hat{\gamma}(h) = 1 - \hat{\rho}(h), \quad (7)$$

where the superscript represents an empirical estimate. Note that there are different alternatives for standardization (e.g., Goda and Atkinson, 2010; Jayaram and Baker, 2010), but results are not significantly affected by a choice with respect to another (e.g., Esposito and Iervolino, 2011).

Normalized-intraevent residuals from multiple events (and regions) are then pooled to fit a unique correlation model. This is because geostatistical estimation needs a relatively large number of data to model the semivariogram (i.e., a number of records to have more than 30 pairs in each h bin), which are not available for individual events in the chosen datasets.

The use of all data implies the assumption of the same isotropic semivariogram with the same parameters for all earthquakes; therefore, the experimental semivariogram becomes that of

$$\hat{\gamma}(h) = \frac{1}{2 \cdot |N(h)|} \cdot \sum_{N(h)} [\varepsilon^*_{pj} - \varepsilon^*_{qj}]^2, \quad (8)$$

where $|N(h)|$ is the number of pairs in the specific h bin from all earthquakes. Note that individual events are kept separated in computing the empirical semivariogram, that is, $\varepsilon^*_{pj} - \varepsilon^*_{qj}$ differences are taken considering only residuals from the same earthquake without mixing up the events.

Spatial Correlation Models of Spectral Accelerations from ESD and ITACA

Analysis and Results

The considered recordings from the ESD data exactly correspond to data used in Esposito and Iervolino (2011); that is, the records (from earthquakes for which more than one record was available) used to fit the Akkar and Bommer (2010) GMPE. For the ITACA dataset, records employed are those used to fit the Bindi *et al.* (2011) GMPE, which is more recent than Bindi *et al.*, (2010), used in the previous study. In particular, the ITACA dataset considered herein is comprised of 763 ground motions from 97 events over the 4–6.9 magnitude range (moment magnitude) and characterized by source-to-site distance (i.e., the closest horizontal distance to the vertical projection of the rupture, the Joyner–Boore distance, R_{jb}) up to 196 km.

In order to have at least 30 pairs per bin and a stable trend of correlation, the experimental semivariograms were obtained using a bin width of 2 km for the ITACA dataset and 4 km for ESD the dataset. (In Esposito and Iervolino [2011], the tolerance bin for ITACA was 1 km due to the much larger dataset used to fit the Bindi *et al.* [2010], GMPE used in that case.) Characteristics of the two datasets and distribution of data pairs as a function of separation distance bins are shown in Figure 1.

For the ESD dataset, the estimation was performed for 9 structural periods ranging between 0.1 s and 2.85 s. Because the GMPE used to obtain intraevent residuals refers to the geometric mean of horizontal components, the correlation was estimated for this IM.

Both classical and robust estimators discussed above were used; no significant differences, as expected, were found in the shape of the experimental semivariogram. The robust estimator was considered to fit the correlation function.

The exponential model was chosen to fit empirical points because this model is widely adopted in literature. Moreover, the choice of using the same model for all periods allows for comparison of results and to investigate the possible dependency of the model parameters on the fundamental period. Assuming that there is no nugget effect (as this study does not investigate variations at a smaller scale with respect to that of the tolerance), the only parameter to estimate is the range b in equation (6). To this aim, LSM was used iteratively (in two stages) to fit the model to the empirical semivariogram. In particular, the range was defined starting from the value estimated by the LSM applied on the semivariogram until a half of the maximum separation distance of residuals in the dataset. The range obtained from this step was then used as an upper bound for the limit distance to apply LSM again on the semivariogram (i.e., until the distance from the first step). This latter step enabled an adjustment of the fitting and obtaining the final practical—range values, that is, the distances at which correlation may be considered to be lost for intraevent residuals of each spectral ordinate.

Following this procedure, the estimated ranges for the exponential models were retrieved for the ESD dataset. Figure 2 shows empirical semivariograms with both estimators and fitted models. For the ITACA dataset, ranges for residuals obtained from Bindi *et al.* (2011) were estimated fitting the exponential model on semivariograms in Figure 3. As a summary, practical ranges for both datasets are given in Table 1.

It should be finally noted that for ITACA, the proposed methodology was used in Esposito and Iervolino (2011) to estimate the horizontal PGA and PGV intraevent residuals' correlation starting from a less recent GMPE and a larger dataset that includes the one used in the present study. As a consistency check, PGA and PGV correlation was reestimated herein. The resulting ranges are very similar to that of the mentioned study; that is, 10.8 km versus 11.5 km for PGA, and 13.7 km versus to 14.5 km for PGV, respectively.

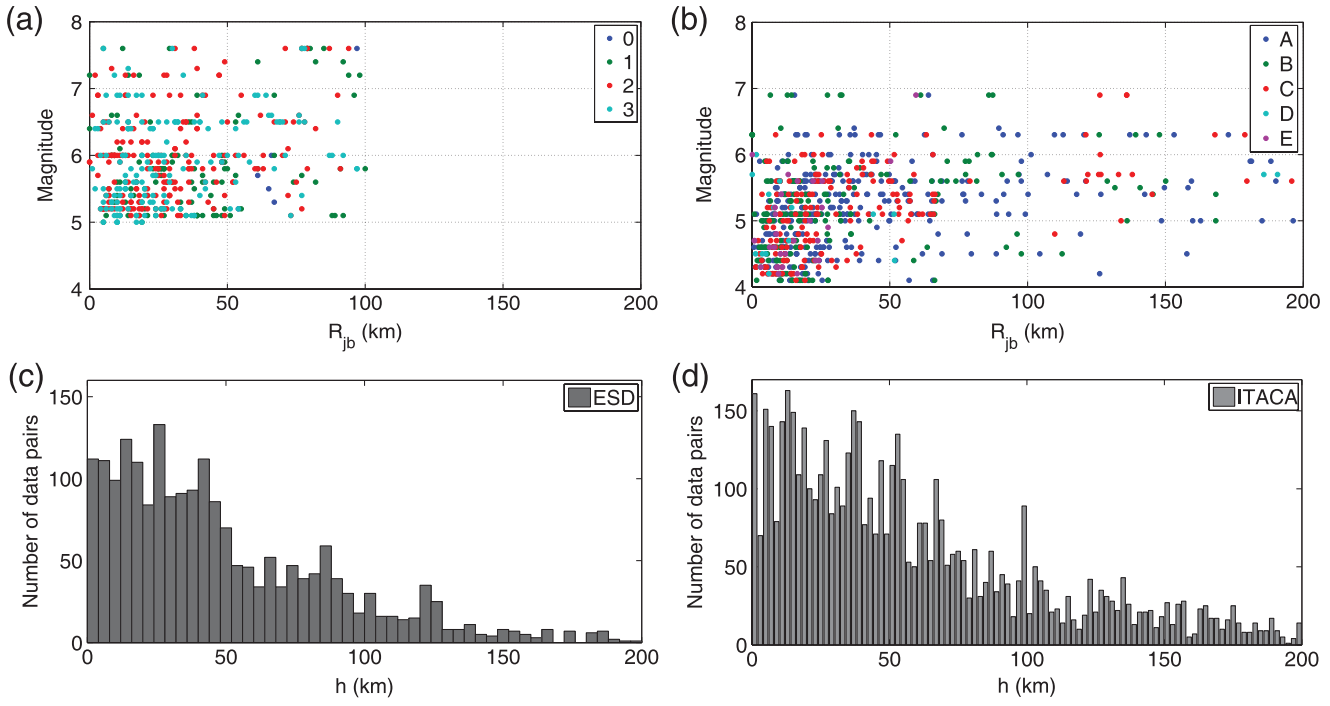

Figure 1. (a) The European Strong-Motion Database subset with respect to magnitude (M), source-to-site distance (R_{jb}) and local site conditions: rock (3), stiff soil (2), soft soil (1), and very soft soil (0); (b) the Italian Accelerometric Archive strong-motion subsets with respect M, R_{jb} and local site conditions according to Eurocode 8 (2004); (c) histograms of the number of data pairs as a function of site-to-site separation distance bin (4 km) for the European dataset; (d) histograms of the number of data pairs as a function of site-to-site separation distance bin (2 km) for the Italian dataset.

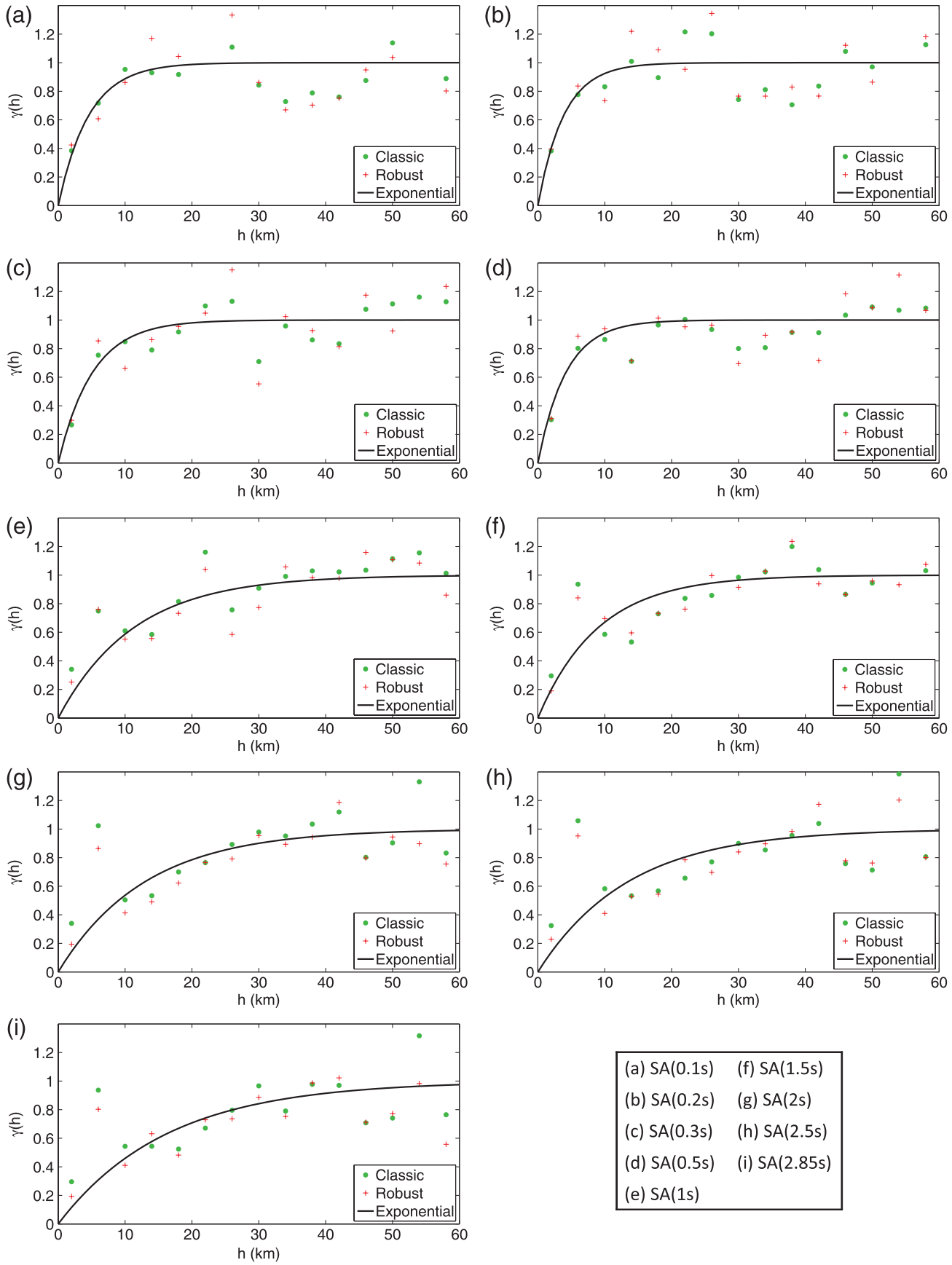

Figure 2. Empirical semivariograms and fitted exponential models for the European Strong-Motion Database.

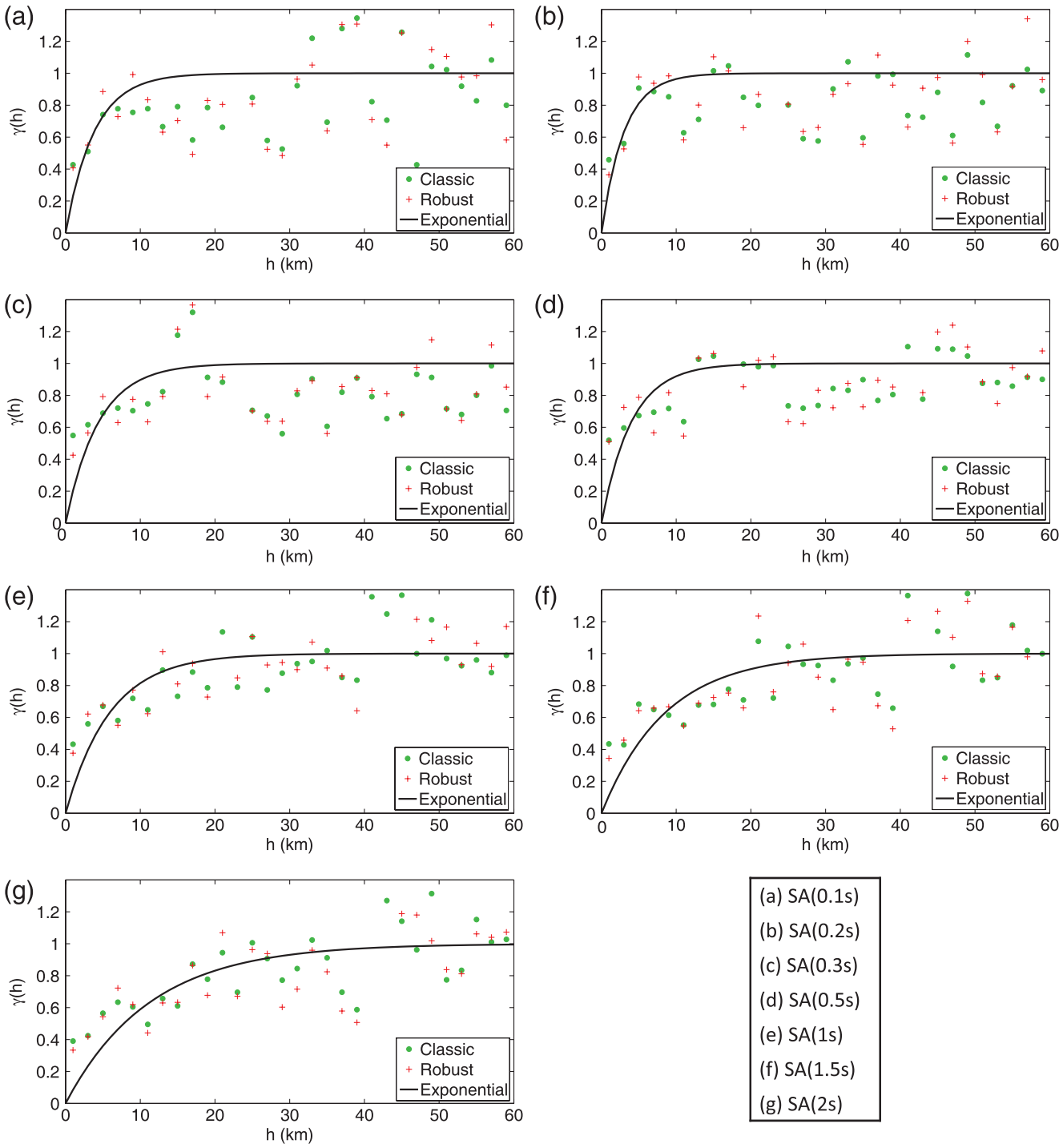

Figure 3. Empirical semivariograms and fitted exponential models for the Italian Accelerometric Archive.

The slight difference may also be related to the bin width used in the estimation of empirical semivariograms (1 km versus 2 km considered herein).

Discussion

Empirical results demonstrate that correlation length tends to increase with period, except for high frequencies at which there is no clear trend. This seems to be consistent with past studies of ground motion coherency (Zerva and Zervas, 2002). In fact, the coherency describes the degree of correlation between amplitudes and phases angles of two-time histories at each of their component frequencies. Considering that coherency decreases with increasing distance between measuring points and with increasing frequency, it may be reasonable to expect more coherent

Table 1
Estimated Ranges for the European Strong-Motion Database (ESD) and the Italian Accelerometric Archive (ITACA)

Dataset	Period (s)	Range (km)
ESD	0.1	13.7
	0.2	11.6
	0.3	15.3
	0.5	12.5
	1	33.9
	1.5	27.0
	2	39.0
	2.5	40.5
	2.85	48.8
ITACA	0.1	11.4
	0.2	9.0
	0.3	13.2
	0.5	11.9
	1	17.8
	1.5	25.7
	2	33.7
	PGA	10.8
	PGV	13.7

ground motion, as SA evaluated at longer periods exhibits more correlated peak amplitudes. This same issue was also discussed in Jayaram and Baker (2009) where generally the estimated ranges increased with period.

Two simple linear-predictive models were fitted using LSM in order to capture the trend of the range (in km) as a function of structural period[2] (in seconds),

$$b(T) = d_1 + d_2 \cdot T, \tag{9}$$

where models parameters d_1 and d_2 are equal to 11.7 and 12.7, respectively, for the ESD dataset and 8.6 and 11.6, respectively, for the ITACA dataset. In Figure 4a these linear functions are shown[3]; thus, based on the results provided, the correlation between normalized intraevent residuals separated by h is obtained as $\rho(h,T) = e^{-3\cdot h/b(T)}$.

Finally, in Figure 4b, to compare results shown herein with existing studies, estimated ranges are compared with some correlation lengths available in literature. Those models were chosen considering the Californian dataset from Goda and Hong (2008), the "all earthquake" model from Hong *et al.* (2009), and the "predictive model" based on all earthquakes from Jayaram and Baker (2009).

Results of this study seem to be comparable with ranges estimated in literature in terms of both trend as a function of vibration period T, and the estimated values of correlation length. It is worth mentioning, for completeness, that an exception in this respect is represented by the Goda and Atkinson (2009, 2010) models in which ranges are larger (never below about 60 km) and the dependence of the correlation on period is not significant.

[2]To fit predictive models, PGA ranges derived in Esposito and Iervolino (2011) for ESD, and herein for ITACA, were included.

[3]Differences among the two datasets appear to be not especially significant; however, they may be attributed to different distributions of magnitude, yet it is difficult to quantitatively investigate this issue because of the relatively small number of records for each magnitude event available.

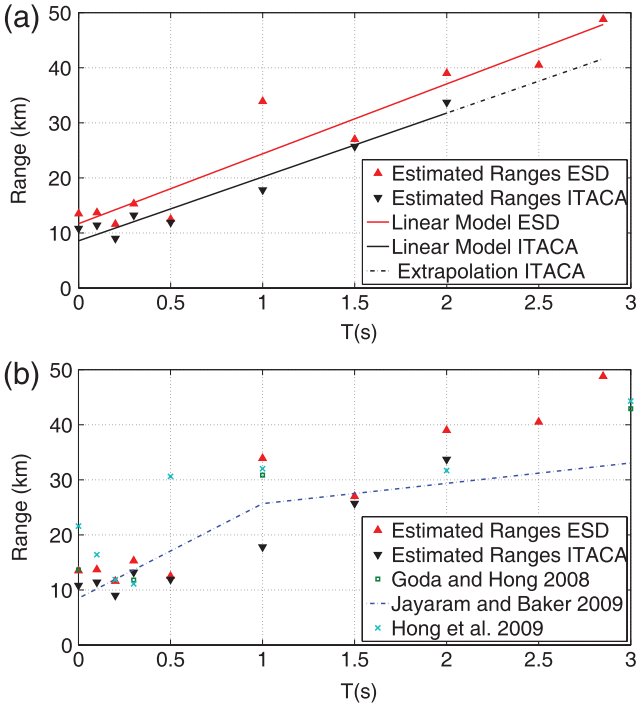

Figure 4. (a) Linear models and estimated ranges for the European Strong-Motion Database (ESD) and for the Italian Accelerometric Archive (ITACA); (b) comparison with available models from literature.

Conclusions

The study presented complements authors' previous work on the assessment of intraevent spatial correlation of residuals of ground-motion intensity measures based on European data. In particular, the focus was elastic SA at periods ranging between 0.1 s and 2.85 s. Subsets of the ITACA and the ESD were used to compute residuals starting from GMPEs calibrated on the same data.

Consistent with the available literature on the topic, hypotheses of stationarity and isotropy of random fields were retained to compute experimental semivariograms of standardized intraevent residuals (with respect to the standard deviation estimated by the GMPEs). Moreover, because only a relatively small number of records for each earthquake were available, records from multiple events and regions were pooled to develop the models.

Exponential correlation models were calibrated from empirical data. The choice of using the same functional form (exponential) for all periods allowed for a comparison of results and the investigation of possible dependency of the parameters on the period. In fact, it was found that practical ranges tend to increase as structural period increases, and simple linear functions were fitted to capture this trend.

Moreover, results were also compared with results from main references on the same topic, finding, in general, consistency.

Starting from the correlation models provided, it is possible to define the joint probability density function for SA(T) at all locations in a region of interest for earthquake engineering and seismic risk assessment applications.

Data and Resources

The ground motions and related information were provided by the authors of Akkar and Bommer (2010) and Bindi *et al.* (2011) GMPEs for ESD (http://www.isesd.hi.is/) and ITACA (http://itaca.mi.ingv.it/ItacaNet/) datasets, respectively. In particular, this study considered subsets of data used to fit these GMPEs; that is, only free field records from earthquakes for which more than one record was available.

Acknowledgments

This study was supported by AMRA scarl (http://www.amracenter.com) under the frame of SYNER-G (7th framework programme of the European Community for research, technological development and demonstration activities; project Contract Number 244061). The authors want to thank Sinan Akkar (Middle East Technical University, Turkey), Dino Bindi (*Deutsches GeoForschungsZentrum*, Germany), and Francesca Pacor (*Istituto Nazionale di Geofisica e Vulcanologia*, Italy) for kindly providing us with datasets used in this study. Finally, the authors acknowledge Associate Editor, Peter Stafford (Imperial College London, United Kingdom), Katsuichiro Goda (University of Bristol, United Kingdom), and an anonymous reviewer for their comments, which improved the quality and readability of the paper.

References

Akkar, S., and J. J. Bommer (2010). Empirical equations for the prediction of PGA, PGV and spectral accelerations in Europe, the Mediterranean Region and the Middle East, *Seismol. Res. Lett.* **81,** no. 2, 195–206.

Barnes, R. J. (1991). The variogram sill and the sample variance, *Math. Geol.* **23,** no. 4, 673–678.

Bindi, D., L. Luzi, and A. Rovelli (2010). Ground motion prediction equations (GMPEs) derived from ITACA. Deliverable No. 14., *Project S4: Italian Strong Motion Data Base*, http://esse4.mi.ingv.it.

Bindi, D., F. Pacor, L. Luzi, R. Puglia, M. Massa, G. Ameri, and R. Paolucci (2011). Ground motion prediction equations derived from the Italian Strong Motion Data Base, *Bull. Earthquake Eng.* **9,** no. 6, 1899–1920.

Boore, D. M., J. F. Gibbs, W. B. Joyner, J. C. Tinsley, and D. J. Ponti (2003). Estimated ground motion from the 1994 Northridge, California, earthquake at the site of the Interstate 10 and La Cienega Boulevard bridge collapse, West Los Angeles, California, *Bull. Seismol. Soc. Am.* **93,** no. 6, 2737–2751.

Cressie, N. (1993). *Statistics for Spatial Data*, Revised Ed., Wiley, New York, 900 p.

Cressie, N., and D. M. Hawkins (1980). Robust estimation of variogram, *Math. Geol.* **12,** no. 2, 115–125.

Esposito, S. (2011). Systemic seismic risk analysis of gas distribution networks. *Ph.D. Thesis*, University of Naples Federico II, Naples, Italy, 178 pp. Available at http://wpage.unina.it/iuniervo/.

Esposito, S., and I. Iervolino (2011). PGA and PGV spatial correlation models based on European multievent datasets, *Bull. Seismol. Soc. Am.* **101,** no. 5, 2532–2541.

Esposito, S., I. Iervolino, and G. Manfredi (2010). PGA semi-empirical correlation models based on European data, in *Proc. of Fourteenth Europ. Conf. Earth. Eng.*, Ohrid, Macedonia, August 30–September 3, Paper no. 998.

Eurocode 8 (2004). Design of structures for earthquake resistance, part 1: General rules, seismic actions and rules for buildings, EN 1998-1, *European Committee for Standardization (CEN)*, http://www.cen.eu/cenorm/homepage.htm.

Goda, K., and G. M. Atkinson (2009). Probabilistic characterization of spatially correlated response spectra for earthquakes in Japan, *Bull. Seismol. Soc. Am.* **99,** no. 5, 3003–3020.

Goda, K., and G. M. Atkinson (2010). Intraevent spatial correlation of ground-motion parameters using SK-net data, *Bull. Seismol. Soc. Am.* **100,** no. 6, 3055–3067.

Goda, K., and H. P. Hong (2008). Spatial correlation of peak ground motions and response spectra, *Bull. Seismol. Soc. Am.* **98,** no. 1, 354–365.

Goovartes, P. (1997). *Geostatistics for Natural Resources Evaluation*, Oxford University Press, New York, 496 p.

Hong, H. P., Y. Zhang, and K. Goda (2009). Effect of spatial correlation on estimated ground motion prediction equations, *Bull. Seismol. Soc. Am.* **99,** no. 2A, 928–934.

Jayaram, N., and J. W. Baker (2008). Statistical tests of the joint distribution of spectral acceleration values, *Bull. Seismol. Soc. Am.* **98,** no. 5, 2231–2243.

Jayaram, N., and J. W. Baker (2009). Correlation model for spatially distributed ground-motion intensities, *Earthquake Eng. Struct. Dynam.* **38,** no. 15, 1687–1708.

Jayaram, N., and J. W. Baker (2010). Considering spatial correlation in mixed-effects regression, and impact on ground-motion models, *Bull. Seismol. Soc. Am.* **100,** no. 6, 3295–3303.

Journel, A. G., and C. J. Huijbregts (1978). *Mining Geostatistics*, Academic Press, London, 600 p.

Malhotra, P. (2008). Seismic design loads from site-specific and aggregate hazard analyses, *Bull. Seismol. Soc. Am.* **98,** no. 4, 1849–1862.

Matheron, G. (1962). *Traité de géostatistique appliquée*, Editions Technip, Paris, France, 333 p (in French).

McGuire, R. K. (2004). *Seismic Hazard and Risk Analysis*, Earthquake Engineering Research Institute, MNO-10, Oakland, California, 178 pp.

Sokolov, V., F. Wenzel, W. Y. Jean, and K. L. Wen (2010). Uncertainty and spatial correlation of earthquake ground motion in Taiwan, *Terr. Atmos. Ocean. Sci.* **21,** no. 6, 905–921.

Zerva, A., and V. Zervas (2002). Spatial variation of seismic ground motion, *App. Mech. Rev.* **55,** no. 3, 271–297.

Dipartimento di Ingegneria Strutturale
Università degli Studi di Napoli Federico II
via Claudio 21
Naples 80125, Italy
simona.esposito@unina.it
iunio.iervolino@unina.it

Manuscript received 26 February 2012